PAUL SCHERRER INSTITUT

ETH zürich

Tobia Claglüna :: AMAS Group, LSM

The Langevin Approach to Discretize the Collision Operator

Master's Thesis Presentation

August 16, 2023

Contact: tobia.clagluena@psi.ch

Outline

Motivation

Motivation

Plasma dynamics in Free Electron Lasers (FELs)

- Accelerated particle bunches emit radiation after passing through undulators
- Particle bunches emit radiation at very short wave lengths (many possible applications)

Motivation

Plasma dynamics in Free Electron Lasers (FELs)

- Accelerated particle bunches emit radiation after passing through undulators
- Particle bunches emit radiation at very short wave lengths (many possible applications)

Problem

- Experiment-Simulation mismatch on energy spread (Prat et al. [2022])
- Energy spread limits bunch compression
- Intrabeam Scattering widens beam
- Existing method for modeling collisions is too expensive (Hockney and Eastwood [2021])

Motivation

Plasma dynamics in Free Electron Lasers (FELs)

- Accelerated particle bunches emit radiation after passing through undulators
- Particle bunches emit radiation at very short wave lengths (many possible applications)

Problem

- Experiment-Simulation mismatch on energy spread (Prat et al. [2022])
- Energy spread limits bunch compression
- Intrabeam Scattering widens beam
- Existing method for modeling collisions is too expensive (Hockney and Eastwood [2021])

Outlook

- Stochastic Ansatz for modeling collisions (Langevin)
- Better computational complexity
- Run solver on an analytical and a real-world test case

Theory

Notation

Table 1: Notation used throughout the presentation.

Symbol	Definition
$\boldsymbol{a}$	Vector quantity $\in \mathbb{R}^3$
$\boldsymbol{a}_i$	Vector component at index i
$\|\boldsymbol{b}\|_2 = \sqrt{\sum_i \lvert b_i \rvert^2}$	L^2-norm
$\underline{\underline{B}}$	Tensor quantity $\in \mathbb{R}^{3\times 3}$
$\underline{\underline{B}}_{i,j}$	Tensor component at index (i, j)
$\underline{\underline{C}} : \underline{\underline{E}}$	$\sum_{i,j} \underline{\underline{C}}_{i,j} \underline{\underline{E}}_{i,j}$
$\nabla_{\boldsymbol{v}}$	Gradient operator acting on velocity space
$\underline{\underline{H}}_{\boldsymbol{v}}$	Hessian operator acting on velocity space

Vlasov-Poisson Equation

Phase Space Definition

$$f(\boldsymbol{r}, \boldsymbol{v}, t) = \frac{1}{\Delta \boldsymbol{r} \Delta \boldsymbol{v}} \int_{\Delta \boldsymbol{r}} d\boldsymbol{r} \int_{\Delta \boldsymbol{v}} d\boldsymbol{v} f_K \quad (1)$$

Vlasov-Poisson Equation

Phase Space Definition

$$f(\boldsymbol{r}, \boldsymbol{v}, t) = \frac{1}{\Delta \boldsymbol{r} \Delta \boldsymbol{v}} \int_{\Delta \boldsymbol{r}} d\boldsymbol{r} \int_{\Delta \boldsymbol{v}} d\boldsymbol{v} f_K \tag{1}$$

Vlasov-Poisson Equation

$$\begin{cases} \dfrac{\partial f}{\partial t} + \boldsymbol{v} \cdot \dfrac{\partial f}{\partial \boldsymbol{r}} + \dfrac{\boldsymbol{F}}{m} \dfrac{\partial f}{\partial \boldsymbol{v}} = \left(\dfrac{\partial f}{\partial t} \right)_{\text{coll}}, \\ \\ \end{cases}$$

Vlasov-Poisson Equation

Phase Space Definition

$$f(\boldsymbol{r}, \boldsymbol{v}, t) = \frac{1}{\Delta \boldsymbol{r} \Delta \boldsymbol{v}} \int_{\Delta \boldsymbol{r}} d\boldsymbol{r} \int_{\Delta \boldsymbol{v}} d\boldsymbol{v} f_K \tag{1}$$

Vlasov-Poisson Equation

$$\begin{cases} \dfrac{\partial f}{\partial t} + \boldsymbol{v} \cdot \dfrac{\partial f}{\partial \boldsymbol{r}} + \dfrac{\boldsymbol{F}}{m} \dfrac{\partial f}{\partial \boldsymbol{v}} = \left(\dfrac{\partial f}{\partial t} \right)_{\text{coll}}, \\ \\ \nabla^2_{\boldsymbol{r}} \phi(\boldsymbol{r}) = -\dfrac{\rho(\boldsymbol{r})}{\epsilon_0}. \end{cases} \tag{2}$$

Vlasov-Poisson Equation

Phase Space Definition

$$f(\boldsymbol{r}, \boldsymbol{v}, t) = \frac{1}{\Delta \boldsymbol{r} \Delta \boldsymbol{v}} \int_{\Delta \boldsymbol{r}} d\boldsymbol{r} \int_{\Delta \boldsymbol{v}} d\boldsymbol{v} f_K \tag{1}$$

Vlasov-Poisson Equation

$$\begin{cases} \dfrac{\partial f}{\partial t} + \boldsymbol{v} \cdot \dfrac{\partial f}{\partial \boldsymbol{r}} + \dfrac{\boldsymbol{F}}{m} \dfrac{\partial f}{\partial \boldsymbol{v}} = \left(\dfrac{\partial f}{\partial t} \right)_{\text{coll}}, \\ \nabla^2_{\boldsymbol{r}} \phi(\boldsymbol{r}) = -\dfrac{\rho(\boldsymbol{r})}{\epsilon_0}. \end{cases} \tag{2}$$

$\rightarrow$ How do we determine the r.h.s. $\left(\frac{\partial f}{\partial t}\right)_{\text{coll}}$?

Scattering in the center of mass frame

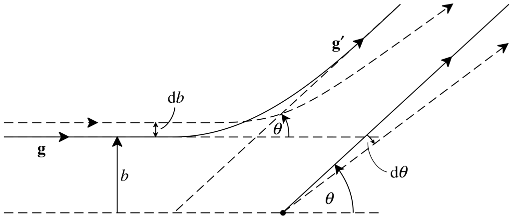

Scattering in the center of mass frame

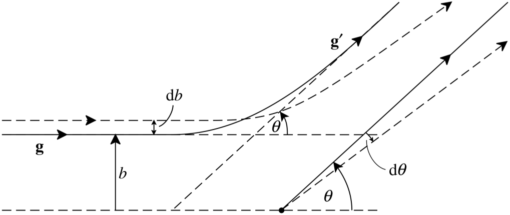

Time Scale of Collisions

$$\tau_c \ll \Delta t \ll \nu \tag{3}$$

Collisions happen **locally** in configuration space (Callen [2018])
$\implies$ can assume collisions solely act on particle velocities

τ_c: Collision Time
ν: Dissipation Time

Fokker-Planck Equation

Fokker-Planck Equation

$$\left(\frac{\partial f}{\partial t}\right)_{\mathsf{coll}} = -\frac{\partial}{\partial \boldsymbol{v}} \cdot \left(f \frac{\langle \Delta \boldsymbol{v} \rangle}{\Delta t}\right) + \frac{1}{2} \frac{\partial^2}{\partial \boldsymbol{v} \partial \boldsymbol{v}} : \left(f \frac{\langle \Delta \boldsymbol{v} \Delta \boldsymbol{v} \rangle}{\Delta t}\right) \tag{4}$$

Fokker-Planck Equation

Fokker-Planck Equation

$$\left(\frac{\partial f}{\partial t}\right)_{\text{coll}} = -\frac{\partial}{\partial \boldsymbol{v}} \cdot \left(f \frac{\langle \Delta \boldsymbol{v} \rangle}{\Delta t}\right) + \frac{1}{2} \frac{\partial^2}{\partial \boldsymbol{v} \partial \boldsymbol{v}} : \left(f \frac{\langle \Delta \boldsymbol{v} \Delta \boldsymbol{v} \rangle}{\Delta t}\right) \tag{4}$$

Collision Coefficients

$$\boldsymbol{F}_d(\boldsymbol{v}) = \frac{\langle \Delta \boldsymbol{v} \rangle}{\Delta t} = \Gamma \frac{\partial h(\boldsymbol{v})}{\partial \boldsymbol{v}}, \tag{5}$$

$$\underline{\underline{D}}(\boldsymbol{v}) = \frac{\langle \Delta \boldsymbol{v} \Delta \boldsymbol{v} \rangle}{\Delta t} = \Gamma \frac{\partial^2 g(\boldsymbol{v})}{\partial \boldsymbol{v} \partial \boldsymbol{v}}. \tag{6}$$

$\boldsymbol{F}_d(\boldsymbol{v})$: Dynamic friction coefficient
$\underline{\underline{D}}(\boldsymbol{v})$: Stochastic diffusion coefficient

Fokker-Planck Equation

Fokker-Planck Equation

$$\left(\frac{\partial f}{\partial t}\right)_{\text{coll}} = -\frac{\partial}{\partial \boldsymbol{v}} \cdot \left(f \frac{\langle \Delta \boldsymbol{v} \rangle}{\Delta t}\right) + \frac{1}{2} \frac{\partial^2}{\partial \boldsymbol{v} \partial \boldsymbol{v}} : \left(f \frac{\langle \Delta \boldsymbol{v} \Delta \boldsymbol{v} \rangle}{\Delta t}\right) \tag{4}$$

Collision Coefficients

$$\boldsymbol{F}_d(\boldsymbol{v}) = \frac{\langle \Delta \boldsymbol{v} \rangle}{\Delta t} = \Gamma \frac{\partial h(\boldsymbol{v})}{\partial \boldsymbol{v}}, \tag{5}$$

$$\underline{\underline{D}}(\boldsymbol{v}) = \frac{\langle \Delta \boldsymbol{v} \Delta \boldsymbol{v} \rangle}{\Delta t} = \Gamma \frac{\partial^2 g(\boldsymbol{v})}{\partial \boldsymbol{v} \partial \boldsymbol{v}}. \tag{6}$$

Poisson Problems (Rosenbluth et al. [1957]).

$$\nabla^2_{\boldsymbol{v}} h(\boldsymbol{v}) = -8\pi f(\boldsymbol{r}, \boldsymbol{v}), \tag{7}$$

$$\nabla^2_{\boldsymbol{v}} \nabla^2_{\boldsymbol{v}} g(\boldsymbol{v}) = -8\pi f(\boldsymbol{r}, \boldsymbol{v}). \tag{8}$$

$\boldsymbol{F}_d(\boldsymbol{v})$:	Dynamic friction coefficient
$\underline{\underline{D}}(\boldsymbol{v})$:	Stochastic diffusion coefficient

Methods

Particle-in-Cell Overview

Electrostatic PIC with **Periodic** boundary conditions.

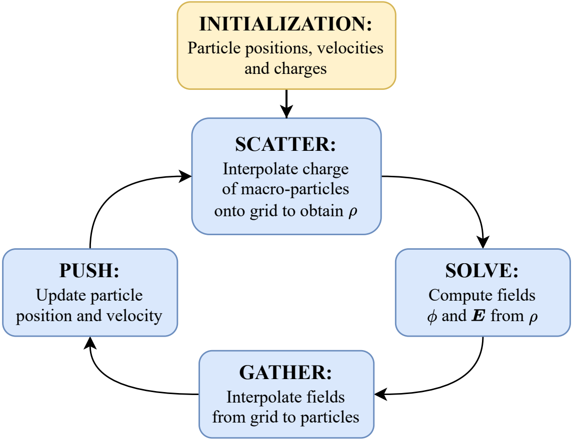

Velocity PIC with **Open** boundary conditions.

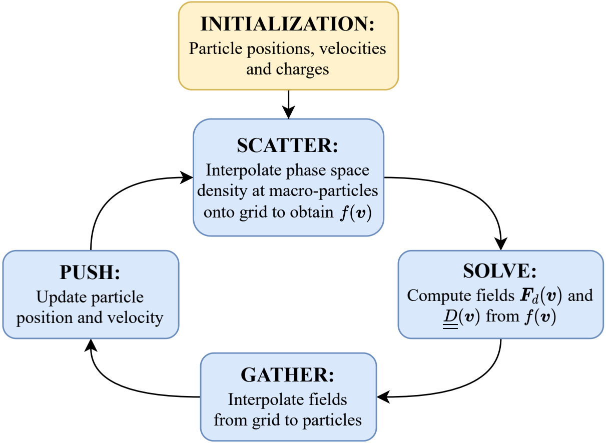

Resulting Scheme

FP Equation $\Longleftrightarrow$ Langevin Equation (Tabar [2019])

$$d\boldsymbol{v}(t) = \underbrace{\boldsymbol{a}(\boldsymbol{v},t)}_{\boldsymbol{F}_d(\boldsymbol{v})}\,dt + \underbrace{\boldsymbol{b}(\boldsymbol{v},t)}_{\underline{\underline{Q}}(\boldsymbol{v})}\,d\boldsymbol{W}(t), \tag{9}$$

$$d\boldsymbol{W}(t) = \boldsymbol{\xi}_t dt, \quad \boldsymbol{\xi}_t \sim \mathcal{N}(0,1). \tag{10}$$

$\boldsymbol{F}_d(\boldsymbol{v})$: Dynamic friction coefficient
$\underline{\underline{D}}(\boldsymbol{v})$: Stochastic diffusion coefficient

Resulting Scheme

FP Equation $\Longleftrightarrow$ Langevin Equation (Tabar [2019])

$$d\boldsymbol{v}(t) = \underbrace{\boldsymbol{a}(\boldsymbol{v},t)}_{\boldsymbol{F}_d(\boldsymbol{v})}\,dt + \underbrace{\boldsymbol{b}(\boldsymbol{v},t)}_{\underline{\underline{Q}}(\boldsymbol{v})}\,d\boldsymbol{W}(t), \tag{9}$$

$$d\boldsymbol{W}(t) = \boldsymbol{\xi}_t dt, \quad \boldsymbol{\xi}_t \sim \mathcal{N}(0,1). \tag{10}$$

LDLT factorization for positive semi-definite Matrices

$$\underline{\underline{D}} = \underline{\underline{LS}}^2\underline{\underline{L}}^T \implies \underline{\underline{Q}} = \underline{\underline{SL}}^T, \tag{11}$$

where $\underline{\underline{D}}$ is positive semi-definite (Hinton [1983]).

$\boldsymbol{F}_d(\boldsymbol{v})$: Dynamic friction coefficient
$\underline{\underline{D}}(\boldsymbol{v})$: Stochastic diffusion coefficient

Resulting Scheme

1: **procedure** ADVANCE PARTICLES IN TIME BY dt
2: $\boldsymbol{r} \leftarrow \boldsymbol{r} + \frac{dt}{2}\boldsymbol{v}$;
3: Compute $\boldsymbol{F}(\boldsymbol{r})$; $\boldsymbol{v} \leftarrow \boldsymbol{v} + \frac{dt}{2}\frac{\boldsymbol{F}}{m}$; (Electrostatic PIC)

Algorithm 1: Euler-Maruyama Time Integrator Procedure.

Resulting Scheme

1: **procedure** ADVANCE PARTICLES IN TIME BY dt
2: $\boldsymbol{r} \leftarrow \boldsymbol{r} + \frac{dt}{2}\boldsymbol{v}$;
3: Compute $\boldsymbol{F}(\boldsymbol{r})$; $\boldsymbol{v} \leftarrow \boldsymbol{v} + \frac{dt}{2}\frac{\boldsymbol{F}}{m}$; (Electrostatic PIC)
4: Compute $\boldsymbol{F}_d(\boldsymbol{v})$ and $\underline{\underline{D}}(\boldsymbol{v})$; (Velocity PIC)

Algorithm 1: Euler-Maruyama Time Integrator Procedure.

Resulting Scheme

1: **procedure** ADVANCE PARTICLES IN TIME BY dt
2: $\boldsymbol{r} \leftarrow \boldsymbol{r} + \frac{dt}{2}\boldsymbol{v}$;
3: Compute $\boldsymbol{F}(\boldsymbol{r})$; $\boldsymbol{v} \leftarrow \boldsymbol{v} + \frac{dt}{2}\frac{\boldsymbol{F}}{m}$; (Electrostatic PIC)
4: Compute $\boldsymbol{F}_d(\boldsymbol{v})$ and $\underline{\underline{D}}(\boldsymbol{v})$; (Velocity PIC)
5: Factorize $\underline{\underline{D}}(\boldsymbol{v})$; $\underline{\underline{Q}} \leftarrow \underline{\underline{SL}}^T$; (LDLT Factorization)

Algorithm 1: Euler-Maruyama Time Integrator Procedure.

Resulting Scheme

procedure ADVANCE PARTICLES IN TIME BY dt

  $\boldsymbol{r} \leftarrow \boldsymbol{r} + \frac{dt}{2}\boldsymbol{v}$;

  Compute $\boldsymbol{F}(\boldsymbol{r})$; $\boldsymbol{v} \leftarrow \boldsymbol{v} + \frac{dt}{2}\frac{\boldsymbol{F}}{m}$; (Electrostatic PIC)

  Compute $\boldsymbol{F}_d(\boldsymbol{v})$ and $\underline{\underline{D}}(\boldsymbol{v})$; (Velocity PIC)

  Factorize $\underline{\underline{D}}(\boldsymbol{v})$; $\underline{\underline{Q}} \leftarrow \underline{\underline{SL}}^T$; (LDLT Factorization)

  $\boldsymbol{v} \leftarrow \boldsymbol{v} + dt\boldsymbol{F}_d + d\boldsymbol{W}(t) \cdot \underline{\underline{Q}}$;

Algorithm 1: Euler-Maruyama Time Integrator Procedure.

Resulting Scheme

procedure ADVANCE PARTICLES IN TIME BY dt
    $\boldsymbol{r} \leftarrow \boldsymbol{r} + \frac{dt}{2}\boldsymbol{v}$;
    Compute $\boldsymbol{F}(\boldsymbol{r})$; $\boldsymbol{v} \leftarrow \boldsymbol{v} + \frac{dt}{2}\frac{\boldsymbol{F}}{m}$; (Electrostatic PIC)
    Compute $\boldsymbol{F}_d(\boldsymbol{v})$ and $\underline{\underline{D}}(\boldsymbol{v})$; (Velocity PIC)
    Factorize $\underline{\underline{D}}(\boldsymbol{v})$; $\underline{\underline{Q}} \leftarrow \underline{\underline{SL}}^T$; (LDLT Factorization)
    $\boldsymbol{v} \leftarrow \boldsymbol{v} + dt\boldsymbol{F}_d + d\boldsymbol{W}(t) \cdot \underline{\underline{Q}}$;
    Compute $\boldsymbol{F}(\boldsymbol{r})$; $\boldsymbol{v} \leftarrow \boldsymbol{v} + \frac{dt}{2}\frac{\boldsymbol{F}}{m}$; (Electrostatic PIC)
    $\boldsymbol{r} \leftarrow \boldsymbol{r} + \frac{dt}{2}\boldsymbol{v}$;
end procedure.

Algorithm 1: Euler-Maruyama Time Integrator Procedure.

Results

Convergence Study: Rosenbluth Potentials

Gaussian Initial Velocity Density

$$f(\boldsymbol{v}) = \frac{1}{\sqrt{8\pi^3}\sigma^3} \exp\left(-\frac{v^2}{2\sigma^2}\right), \quad \sigma = 0.05 v_{max} \tag{12}$$

Relative approximation error η

$$\eta(x, x_{\mathsf{appr}}) = \frac{\|x_{\mathsf{appr}} - x\|_2}{\|x\|_2} \tag{13}$$

Convergence Study: Rosenbluth Potentials

Gaussian Initial Velocity Density

$$f(\boldsymbol{v}) = \frac{1}{\sqrt{8\pi^3}\sigma^3} \exp\left(-\frac{v^2}{2\sigma^2}\right), \quad \sigma = 0.05 v_{max} \tag{14}$$

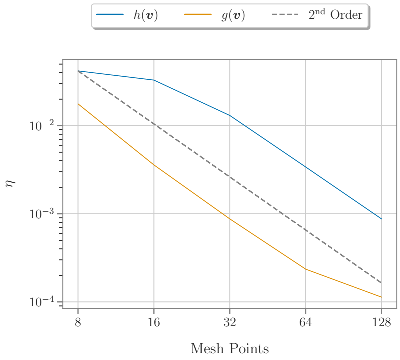

Convergence Study: Rosenbluth Potentials

Gaussian Initial Velocity Density

$$f(\boldsymbol{v}) = \frac{1}{\sqrt{8\pi^3}\sigma^3} \exp\left(-\frac{v^2}{2\sigma^2}\right), \quad \sigma = 0.05 v_{max} \tag{14}$$

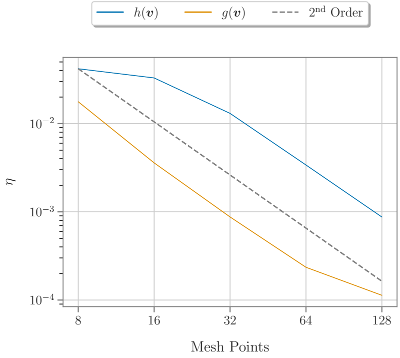

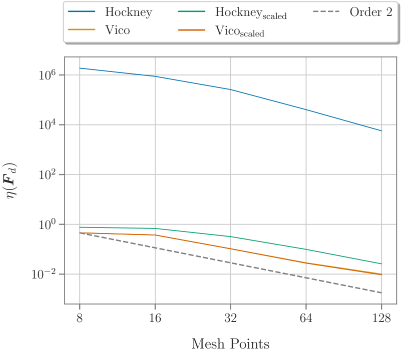

Disorder Induced Heating (DIH) Test Case

Disorder Induced Heating (DIH) Test Case

P^3M Reference Implementation

- $P^3M \equiv$ (Particle-Particle Particle-Mesh) by Hockney and Eastwood [2021], Ulmer [2016]
- High computational complexity
- 2 hyperparameters (cut-off radius r_c, interaction splitting parameter α)

Disorder Induced Heating (DIH) Test Case

P^3M Reference Implementation

- $P^3M \equiv$ (Particle-Particle Particle-Mesh) by Hockney and Eastwood [2021], Ulmer [2016]
- High computational complexity
- 2 hyperparameters (cut-off radius r_c, interaction splitting parameter α)

Cold Sphere Initial Condition (Mitchell et al. [2015])

- $N_p = 156055$ electrons in a sphere of radius $R = 17.74\ \mu m \implies \tau_p = 4.31 \times 10^{-11}\ s$
- Simulation time: $t_{tot} = 5\tau_p$, $dt = 2.15623 \times 10^{-13}\ s \implies 1000\ dt$
- Particles initially at rest: $\boldsymbol{v}(t = 0) = 0$
- Normalized x-emittance at equilibrium: $\varepsilon_{x,n} = 0.491\ nm$

τ_p:	Plasma period
$\varepsilon_{x,n}$:	Normalized x-emittance

Disorder Induced Heating (DIH) Test Case

Solver setup for the DIH experiments:

PIC Type	Quantity of Interest	Comp. Domain or Method
Electrostatic PIC	$-\nabla_{\boldsymbol{r}}\left[\phi(\boldsymbol{r})\right]$	Spectral Gradient: $\nabla_{\boldsymbol{r}}^{\mathsf{sp}}$
Velocity PIC	$\nabla_{\boldsymbol{v}} h(\boldsymbol{v}),\ g(\boldsymbol{v})$	Vico et al. [2016] + $\nabla_{\boldsymbol{v}}^{\mathsf{sp}}$
	$\frac{\partial^2}{\partial \boldsymbol{v} \partial \boldsymbol{v}} g(\boldsymbol{v})$	FD Hessian: $\underline{\underline{H}}_{\boldsymbol{v}}^{\mathsf{fd}}$

$\star^{\mathsf{fd}}$: Operator computed with Finite Difference (FD)
$\star^{\mathsf{sp}}$: Operator computed with a spectral method (Vico et al. [2016])

Normalized x-emittance $\varepsilon_{x,n}$ of collisionless Langevin solver and P^{3}M .

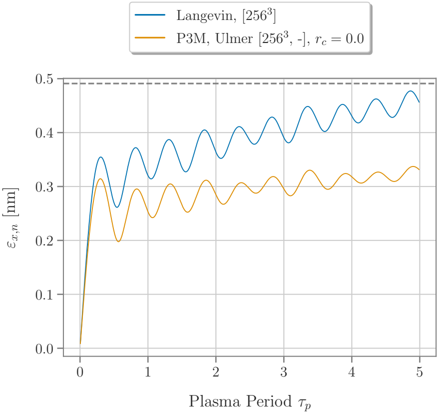

Friction & Diffusion Coefficient

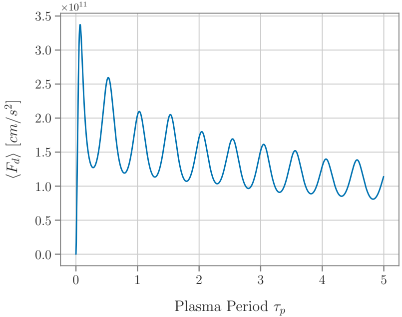

Friction & Diffusion Coefficient

- Friction coefficients on their own are not large enough to impact $\varepsilon_{x,n}$.

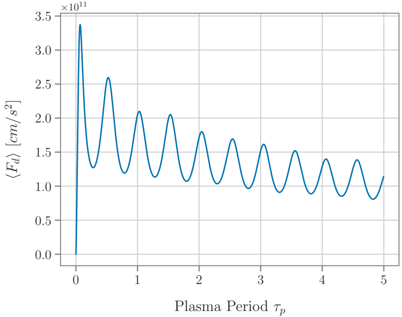

Friction & Diffusion Coefficient

- Friction coefficients on their own are not large enough to impact $\varepsilon_{x,n}$.
- Diagonal diffusion coefficients are indeed dominant (Manheimer et al. [1997]).

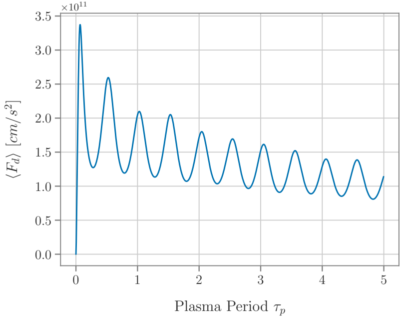

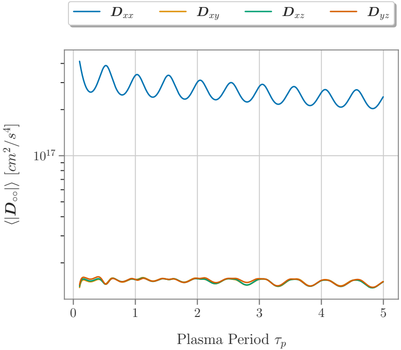

Friction & Diffusion Coefficient

- Friction coefficients are too small to impact $\varepsilon_{x,n}$.
- Diagonal diffusion coefficients are indeed dominant (Manheimer et al. [1997]).
- Off-diagonal values show non-periodic behavior for $t < 3\tau_p$.

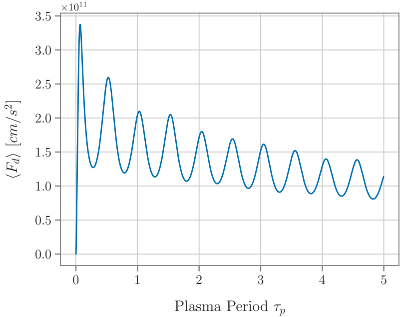

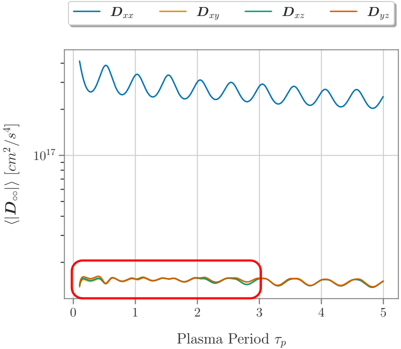

Investigation of Diffusion Coefficients $\underline{\underline{D}}$

- Diffusion matrices not only positive semi-definite (inhibits LDLT decomposition)

Investigation of Diffusion Coefficients $\underline{\underline{D}}$

- Diffusion matrices not only positive semi-definite (inhibits LDLT decomposition)

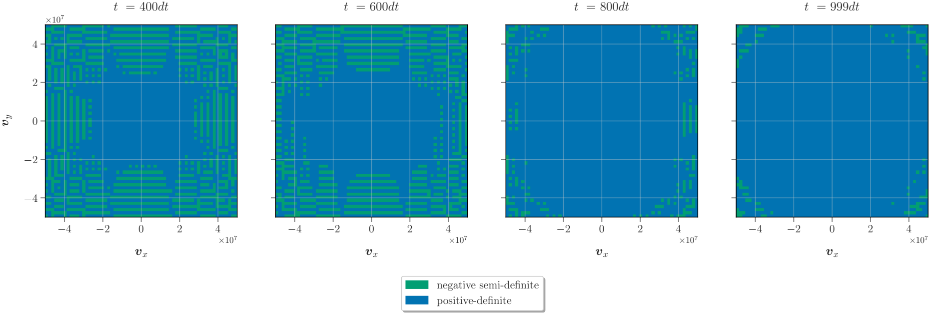

Investigation of Diffusion Coefficients $\underline{\underline{D}}$

- Diffusion matrices not only positive semi-definite (inhibits LDLT decomposition)
- Negative definite matrices start to vanish after $t = 3\tau_p$

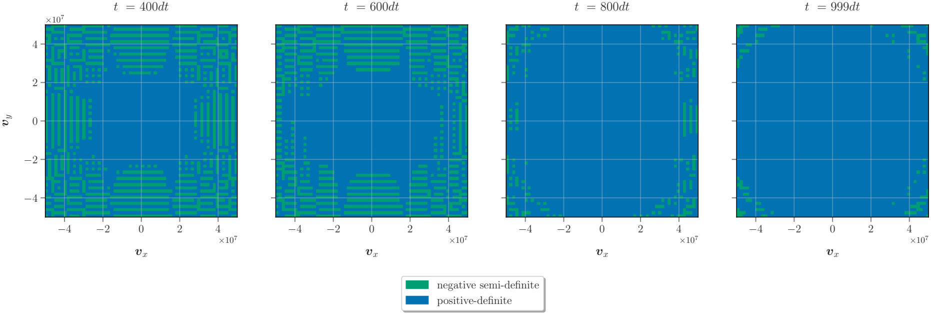

Summary

Conclusion

Langevin Solver for the Vlasov-Poisson-Vokker-Planck equation

- Better complexity than reference solver (P^3M) / less hyperparameters

Conclusion

Langevin Solver for the Vlasov-Poisson-Vokker-Planck equation

- Better complexity than reference solver (P^3M) / less hyperparameters
- Verified correctness of collision operator on analytical test cases

Conclusion

Langevin Solver for the Vlasov-Poisson-Vokker-Planck equation

- Better complexity than reference solver (P^3M) / less hyperparameters
- Verified correctness of collision operator on analytical test cases
- Investigated impact of two solver types on normalized emittance

Conclusion

Langevin Solver for the Vlasov-Poisson-Vokker-Planck equation

- Better complexity than reference solver (P^3M) / less hyperparameters
- Verified correctness of collision operator on analytical test cases
- Investigated impact of two solver types on normalized emittance
- Friction coefficient exhibits no impact on DIH test case

Conclusion

Langevin Solver for the Vlasov-Poisson-Vokker-Planck equation

- Better complexity than reference solver (P^3M) / less hyperparameters
- Verified correctness of collision operator on analytical test cases
- Investigated impact of two solver types on normalized emittance
- Friction coefficient exhibits no impact on DIH test case
- Negative definite diffusion matrices inhibit adding diffusive term in time integration

Conclusion

Outlook

- Investigate noise in diffusion matrices for $t < 3\tau_p$

h_v: Mesh width in velocity space

Conclusion

Outlook

- Investigate noise in diffusion matrices for $t < 3\tau_p$
- Investigate dt/h_v interplay in the symmetric time integrator (i.e. subcycling)

h_v: Mesh width in velocity space

Conclusion

Outlook

- Investigate noise in diffusion matrices for $t < 3\tau_p$
- Investigate dt/h_v interplay in the symmetric time integrator (i.e. subcycling)
- Test convserving time integrator (high order SDE methods)

h_v: Mesh width in velocity space

Conclusion

Outlook

- Investigate noise in diffusion matrices for $t < 3\tau_p$
- Investigate dt/h_v interplay in the symmetric time integrator (i.e. subcycling)
- Test convserving time integrator (high order SDE methods)
- Test on a simpler physical test case

h_v: Mesh width in velocity space

Conclusion

Outlook

- Investigate noise in diffusion matrices for $t < 3\tau_p$
- Investigate dt/h_v interplay in the symmetric time integrator (i.e. subcycling)
- Test convserving time integrator (high order SDE methods)
- Test on a simpler physical test case
- Performance improvements:
  - Asynchronous computation of $\boldsymbol{F}_d(\boldsymbol{v})$ and $\underline{\underline{D}}(\boldsymbol{v})$
  - MPI parallelization via "Super-Cell" approach (Qiang et al. [2000])

h_v: Mesh width in velocity space

Appendix

Appendix I: Explored Solver components

Possible ways of defining the electrostatic Poisson problem:

$$\nabla^2 \phi(\boldsymbol{r}) = -\frac{\rho(\boldsymbol{r})}{\varepsilon_0}$$

$$\phi(\boldsymbol{r}) = \int G(\boldsymbol{r}, \boldsymbol{r}')\rho(\boldsymbol{r})dV', \quad \text{Definition I}$$

$$\hat{\phi}(\boldsymbol{\xi}) = \frac{\hat{\rho}(\boldsymbol{\xi})}{k^2 \varepsilon_0}, \quad \text{Definition II}$$

PIC Type	**Quantity of Interest**	**Comp. Domain or Method**
Electrostatic PIC	$\phi(\boldsymbol{r})$	Definition I (see Fig. above)
		Definition II (see Fig. above)
	$-\nabla_{\boldsymbol{r}} \phi(\boldsymbol{r})$	Finite Difference Gradient: $\nabla_{\boldsymbol{r}}^{\text{fd}}$
		Spectral Gradient: $\nabla_{\boldsymbol{r}}^{\text{sp}}$
Velocity PIC	$\nabla_{\boldsymbol{v}} h(\boldsymbol{v}),\ g(\boldsymbol{v})$	Hockney, $\nabla_{\boldsymbol{v}}^{\{\text{fd,sp}\}}$
		Vico, $\nabla_{\boldsymbol{v}}^{\{\text{fd,sp}\}}$
	$\frac{\partial^2}{\partial \boldsymbol{v} \partial \boldsymbol{v}} g(\boldsymbol{v})$	Finite Difference Hessian: $\underline{\underline{H}}_{\boldsymbol{v}}^{\text{fd}}$
		Spectral Hessian: $\underline{\underline{H}}_{\boldsymbol{v}}^{\text{sp}}$

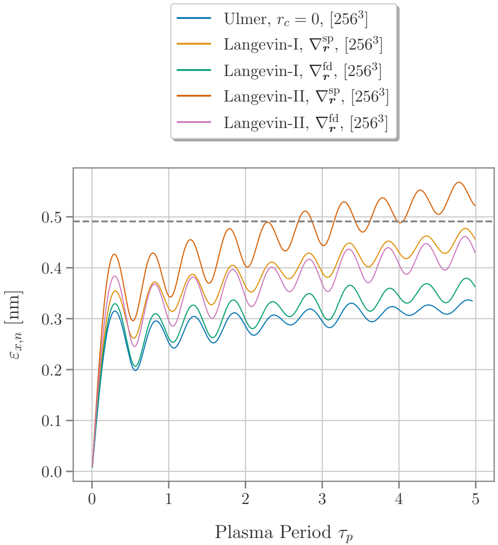
Ulmer, $r_c = 0$, $[256^3]$
Langevin-I, $\nabla_{\boldsymbol{r}}^{\mathrm{sp}}$, $[256^3]$
Langevin-I, $\nabla_{\boldsymbol{r}}^{\mathrm{fd}}$, $[256^3]$
Langevin-II, $\nabla_{\boldsymbol{r}}^{\mathrm{sp}}$, $[256^3]$
Langevin-II, $\nabla_{\boldsymbol{r}}^{\mathrm{fd}}$, $[256^3]$
$\varepsilon_{x,n}$ [nm]
0.0
0.1
0.2
0.3
0.4
0.5
0
1
2
3
4
5
Plasma Period τ_p

Appendix III: Varying Poisson Solver Mesh Size

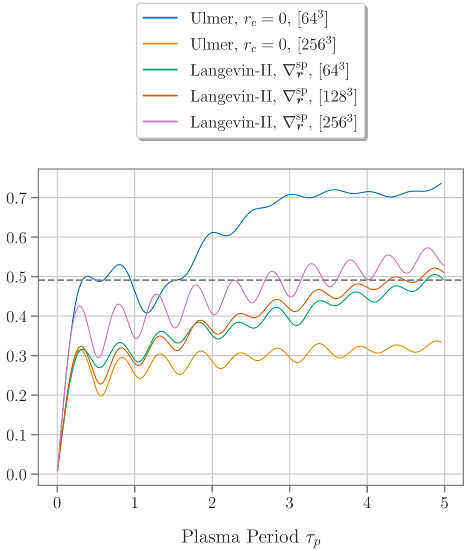

Convergence study of collisional coefficients for a Gaussian velocity distribution which models the distribution of the dih problem.

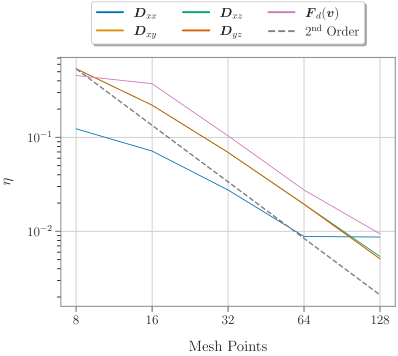

(a) Finite Difference computation of coefficients.

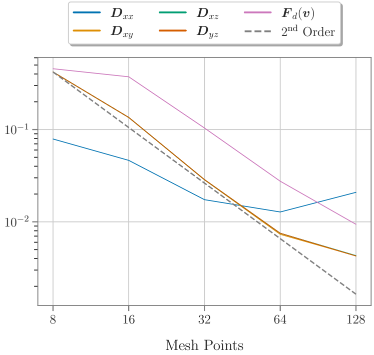

(b) Spectral computation of coefficients.

Appendix V: Friction & Diffusion Coefficients

Friction coefficient does not have any impact on DIH $\varepsilon_{x,n}$:

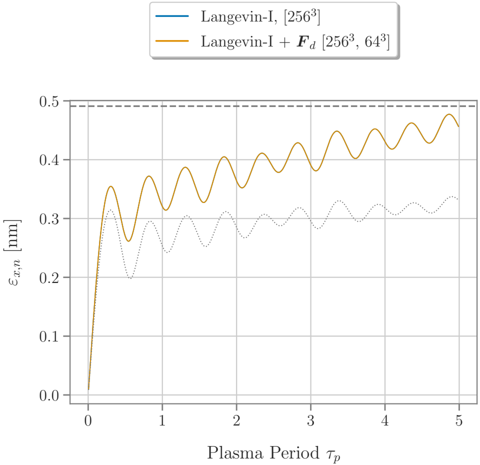

Appendix VI: Chainable differential operators

Listing 1: Pseudo-code for a chained operator (equivalent to $\frac{\partial^2}{\partial x \partial y} f(x, y)$).

```
constexpr int Dim = 2;

typedef double T;
// Inverse mesh-spacing
ippl::Vector<Dim, T> hInv = {40.0, 40.0};

// Field of type double and size [100]^2
Field<Dim, T> field(100, 100, 1.0 / hInv);

// Define the stencils applied along the x and y dimension
DiffType DiffX = DiffType::Forward;
DiffType DiffY = DiffType::Backward;

// Operator that is applied first
typedef DiffOpChain<OpDim::Y, Dim, T, DiffY, FView_t> firstOperator;
// Operator that is applied after the first
DiffOpChain<OpDim::X, Dim, T, DiffX, firstOperator> diff_xy(field, hInv);

// Compute curvature at index (42,42)
double result = diff_xy(42, 42);
```

Appendix VII: Chainable differential operators

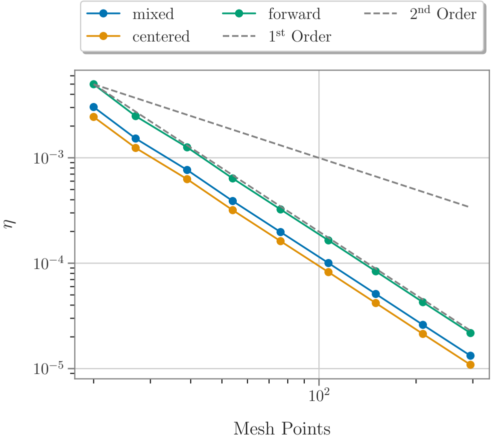

Appendix VII: Computational Complexity

$$C_{\mathsf{P^3M}}\,(N_p, N_m, \delta) = \underbrace{\mathcal{O}(N_p^2\delta^3)}_{\text{Particle-Particle}} + \underbrace{\mathcal{O}(N_p) + \mathcal{O}(N_m \log(N_m))}_{\text{Particle-Mesh}}, \tag{15}$$

$$\begin{aligned} C_{\mathsf{Langevin}}(N_p, N_m) &= \underbrace{\mathcal{O}(N_p) + \mathcal{O}(N_m \log(N_m))}_{\boldsymbol{F}_d} \\ &+ \underbrace{\mathcal{O}(N_p) + \mathcal{O}(N_m) + \mathcal{O}(N_m \log(N_m))}_{\underline{\underline{D}}} \\ &+ \underbrace{\mathcal{O}(N_p) + \mathcal{O}(N_m \log(N_m))}_{\text{Particle-Mesh}} \\ &= \mathcal{O}(N_p) + \mathcal{O}(N_m \log(N_m)). \end{aligned} \tag{16}$$

$\delta = r_c/L$ is the ratio of the cut-off radius r_c w.r.t. the domain length L.

Appendix VIII: Energy Spread (Prat et al. [2022])

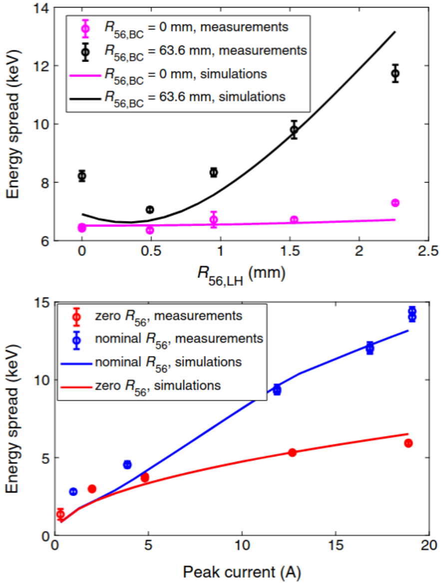

References I

Eduard Prat, Paolo Craievich, Philipp Dijkstal, Simone Di Mitri, Eugenio Ferrari, Thomas G Lucas, Alexander Malyzhenkov, Giovanni Perosa, Sven Reiche, and Thomas Schietinger. Energy spread blowup by intrabeam scattering and microbunching at the SwissFEL injector. *Physical Review Accelerators and Beams*, 25(10):104401, 2022. URL `https://doi.org/10.1103/PhysRevAccelBeams.25.104401`.

R.W Hockney and J.W Eastwood. *Computer Simulation Using Particles*. CRC Press, March 2021. doi: 10.1201/9780367806934. URL `https://doi.org/10.1201/9780367806934`. ISBN: 978-0-367-80693-4.

James D. Callen. *Plasma Kinetic Theory*, chapter Coulomb Collision Operator. 2018. URL `https://drive.google.com/file/d/1j2Afyq1DO2zeyFf9qTTfFVL9F9Rxzn7s/view?pli=1`. Accessed: 2023-01-29.

Marshall N. Rosenbluth, William M. MacDonald, and David L. Judd. Fokker-Planck equation for an inverse-square force. *Phys. Rev.*, 107:1–6, Jul 1957. doi: 10.1103/PhysRev.107.1. URL `https://link.aps.org/doi/10.1103/PhysRev.107.1`.

M. Reza Rahimi Tabar. *Equivalence of Langevin and Fokker–Planck Equations*, pages 61–68. Springer International Publishing, Cham, 2019. ISBN 978-3-030-18472-8. doi: 10.1007/978-3-030-18472-8_7. URL `https://doi.org/10.1007/978-3-030-18472-8_7`.

References II

Fred L Hinton. Collisional transport in plasma. *Handbook of Plasma Physics*, 1(147): 331, 1983. ISBN: 0-444-86645-0.

Benjamin Ulmer. The P3M Model on Emerging Computer Architectures With Application to Microbunching. Master's thesis, ETH Zürich, 2016. URL `https://amas.web.psi.ch/people/aadelmann/ETH-Accel-Lecture-1/projectscompleted/cse/thesisBUlmer.pdf`.

Chad Mitchell, Ji Qiang, et al. A Parallel Particle-Particle, Particle-Mesh Solver for Studying Coulomb Collisions in the Code IMPACT-T. In *6th Int. Particle Accelerator Conf.(IPAC'15), Richmond, VA, USA , May 3-8, 2015*, pages 593–595. JACOW, Geneva, Switzerland, 2015. URL `https://accelconf.web.cern.ch/IPAC2015/papers/mopma024.pdf`.

Felipe Vico, Leslie Greengard, and Miguel Ferrando. Fast Convolution with Free-Space Green's Functions. *Journal of Computational Physics*, 323:191–203, 2016. ISSN 0021-9991. doi: https://doi.org/10.1016/j.jcp.2016.07.028. URL `https://www.sciencedirect.com/science/article/pii/S0021999116303230`.

Wallace M Manheimer, Martin Lampe, and Glenn Joyce. Langevin representation of Coulomb collisions in PIC simulations. *Journal of Computational Physics*, 138(2): 563–584, 1997.

Ji Qiang, Robert D Ryne, and Salman Habib. Self-consistent Langevin simulation of Coulomb collisions in charged-particle beams. In *SC'00: Proceedings of the 2000 ACM/IEEE Conference on Supercomputing*, pages 27–27. IEEE, 2000.